Catalysis Today 166 (2011) 67–72

Contents lists available at ScienceDirect

Catalysis Today

journal homepage: www.elsevier.com/locate/cattod

WO_3 microcrystallites: One of the crucial factors controlling the isomerization activity of $Pt/WO_3–ZrO_2$

Yueqin Song[a], Juanjuan Zhang[a], Xiaolong Zhou[a,*], Jin-An Wang[b], Longya Xu[c], Guoxian Yu[d]

[a] Petroleum Processing Research Center, East China University of Science and Technology, Shanghai 200237, PR China
[b] Laboratorio de Catálisis y Materiales, ESIQIE, Instituto Politécnico Nacional, Col. Zacatenco, 07738, México, D.F., Mexico
[c] State Key Laboratory of Catalysis, Dalian Institute of Chemical Physics, the Chinese Academy of Sciences, Dalian, Liaoning 116023, PR China
[d] School of Chemistry and Environment Engineering, Jianghan University, Wuhan, Hubei Province 430056, PR China

ARTICLE INFO

Article history:
Available online 5 July 2010

Keywords:
Hydrothermal
Hydrous zirconia
Platinum
Tungstated zirconia
n-Hexane
Isomerization

ABSTRACT

A series of hydrous zirconia supports were prepared by hydrothermal method and $Pt/WO_3–ZrO_2$ catalysts were prepared by impregnation method. The catalytic activity of $Pt/WO_3–ZrO_2$ in n-hexane isomerization was evaluated in a fixed-bed reactor. In order to investigate the crystalline structure, acidity, and textural properties, the catalysts were characterized by XRD and Raman spectroscopy, NH_3-TPD, FTIR, and N_2 adsorption. The results indicated that the crystalline structure of hydrous zirconia support and the state of tungsten oxide species over the catalyst varied obviously with the hydrothermal temperature, while no distinct change in the acidity of the catalyst occurred. The isomerization activity of $Pt/WO_3–ZrO_2$ could not well be correlated with the crystalline structure of hydrous zirconia support and the acidity. It was proposed that the presence of considerable microcrystalline WO_3 in catalyst was indispensable for achieving high isomerization activity.

1. Introduction

The commercialization of $Pt/Cl\text{-}Al_2O_3$ and Pt/zeolites metal-acid bi-functional catalysts has been achieved in the skeletal isomerization of n-pentane/n-hexane in the petrochemical industries in the last century. In recent years, many investigations have been intensely focused on the strong acid catalysts like Pt-promoted sulfated zirconia or tungstated zirconia, aiming towards a breakthrough in the development of new generation of environmentally friendly solid acid catalysts [1–8]. For the $WO_3–ZrO_2$ based catalysts, there still exist some controversy regarding the relationship between the surface acidity, crystalline structure and catalytic performance [3,4,9–11]. Hwang et al. [9,10] considered that the isomerization activity of tungstated zirconia was determined by its strong acid sites. However, other researchers reported that the catalytic activity was independent of the acidity of tungstated zirconia and was related to the redox properties of WO_X or the formation of W^{5+} species [12–14]. It is generally accepted that tungstated zirconia catalyst with or without Pt-promotion possessed strong acidity and high isomerization activity only when the hydrous zirconia support was amorphous [2,15]. However, the recent investigation from Huang et al. [11] indicated that $WO_3–ZrO_2$ using tetragonal zirconia as support prepared by supercritical drying method, showed almost comparable n-alkane conversion activity to the catalyst prepared from amorphous hydrous zirconia. Our previous investigation also indicated that that $Pt/WO_3–ZrO_2$ using amorphous hydrous zirconia as support possessed very lower isomerization activity than that using crystalline hydrous zirconia [16]. The catalytic activity could not correlated with the acidity, crystalline structure of the catalyst. Maybe, the state of tungsten oxide over the catalyst would influence the catalytic activity. Up to now, seldom investigations have been carried out to elucidate the role of WO_3 microcrystallites in determining the catalytic activity of $Pt/WO_3–ZrO_2$.

In the present work, we prepared Pt-promoted tungstated zirconia catalysts with different acidities, crystalline structures and different tungsten oxide species in order to clarify whether the state of tungsten oxide played an important role in determining the catalytic activity. Particular emphasis was given to the role of WO_3 microcrystallites over $Pt/WO_3–ZrO_2$ in the hydroisomerization reaction of n-hexane.

2. Experimental

2.1. Preparation of zirconia support and catalysts

Firstly, $ZrO(NO_3)_2$ aqueous solution of 0.4 M was added dropwise into NH_3 solution of 2.5 wt% while vigorously stirring and the

* Corresponding author at: Petroleum Processing Research Center, East China University of Science and Technology, No 130, Meilong Road, Shanghai 200237, PR China. Tel.: +86 21 64252041; fax: +86 21 64252041.
E-mail addresses: yqsong@mail.tsinghua.edu.cn (Y. Song), zj6083@yahoo.com.cn (J. Zhang), xiaolong@ecust.edu.cn (X. Zhou), jwang@ipn.mx (J.-A. Wang), lyxu@dicp.ac.cn (L. Xu), guoxianyu828@yahoo.com.cn (G. Yu).

0920-5861/$ – see front matter © 2010 Elsevier B.V. All rights reserved.
doi:10.1016/j.cattod.2010.05.037

final pH value of the slurry was 10. After the precipitation, stirring continued for 0.5 h and then the white precipitate of $Zr(OH)_4$ was aged in the mother liquid at room temperature for 10 h. The precipitate was filtered and washed thoroughly with deionized water till the pH value of the filtrate was ca. 7. The obtained hydro-gel was evenly mixed with distilled water under vigorous stirring and the formed slurry (pH 7) was transferred into a stainless Teflon-lined 100 ml capacity autoclave and underwent the hydrothermal process at a given temperature for 30 h. After that, the autoclave was admitted to cool to room temperature. The hydrous zirconia after the hydrothermal treatment was filtered and was dried at 110 °C for 12 h in air, which was denoted as Zr-T, where *T* represents hydrothermal temperature (°C).

Addition of tungsten and platinum: W was introduced into the obtained hydrous zirconia supports by impregnating with ammonium meta-tungstate. The samples loaded with W were dried at 110 °C and calcined at 700 °C in air for 3 h, denoted as WZr-T. The samples loaded with W after calcination at 750 °C and 800 °C, respectively were denoted as WZr-Ta and WZr-Tb. PWZr-T catalysts were prepared by impregnating WZr-T with hexachloroplatinic (IV) acid solution and then calcined at 500 °C in air for 3 h. The loadings of tungsten oxide and platinum were 15 wt% and 0.5 wt%, respectively.

2.2. Catalyst characterization

X-ray diffraction (XRD) patterns were obtained on a Philips MagiX X-ray diffractometer, using Cu $K\alpha_1$ radiation at room temperature and instrumental settings of 40 kV and 40 mA. The scanning was within a range of 2θ from 10° to 70° at a scanning rate of 6° min^{-1}.

N_2 adsorption and desorption isotherm experiments were performed in liquid nitrogen at −196 °C on the NOVA 4000 gas adsorption analyzer (Quantachrome Corp.). Each sample was evacuated at 200 °C for 5 h before N_2 adsorption. The total surface area was calculated according to the BET isothermal equation and the pore distribution was obtained according to BJH method.

H_2-temperature programmed reduction (H_2-TPR) was carried out on a TP5000 multi-functional adsorption equipment. The sample (0.1 g) was first pretreated in a flow of He at 400 °C for 30 min and then was cooled to room temperature. Subsequently, the sample was again heated from ambient temperature to 700 °C in a 5% H_2/N_2 flow (30 ml/min) at a heating rate of 10 °C/min.

Raman spectra were obtained on Microscopic Confocal RM2000 Raman Spectrometer (Renishaw Corp.) at room temperature and atmospheric pressure. The exciting wavelength of 514.5 nm was generated with an Arlaser with a power of 15 mW and a spot size of ca. 3 μm^2. The laser beam was focused on the top of the catalyst.

Pyridine adsorption infra-red (Py-IR) was carried out on an EQUIOX 55 Fourier transform infra-red spectrometer (Bruker Corp.). Self-supporting wafers of the samples (ca. 10 mg, 10 mm diameter) were loaded on the IR cell. The wafer was evacuated 400 °C and then cooled down to room temperature for the record of background spectra. The wafer was saturated with pyridine, evacuated at 150 °C for 0.5 h and then again cooled to room temperature. FTIR spectra were recorded at a spectra resolution of 2 cm^{-1} with the subtraction of the sample background. Then, the wafer was evacuated at 350 °C for 0.5 h and then again cooled to room temperature. The FTIR spectra were recorded following the above procedure.

2.3. Catalytic activity measurement

The isomerization reaction of n-hexane (AR) was carried out in a continuous flow fixed-bed stainless steel reactor (i.d. = 5 mm). Before the reaction, the catalyst was pretreated in a flow of drying air at 450 °C for 3 h to remove the impurity such as hydrocarbon and water adsorbed on the catalyst surface. After that, the catalyst bed was cooled to 280 °C and reduced in a flow of hydrogen (20 ml/min) for 2 h. Subsequently, the temperature of the catalyst was decreased to a given value, and hydrogen and n-hexane were simultaneously introduced into the reactor. The molar ratio of H_2/n-hexane was 30, reaction pressure was 2 MPa, and weight hourly space velocity (WHSV) was 1 h^{-1}. The flow rate of n-hexane and hydrogen was controlled using a double column pump and a mass flow meter, respectively. The products were analyzed on-line by GC-920 (provided by Shanghai Institute of Computer Technology), equipped with an FID and an OV-101capillary column.

3. Results

3.1. Crystalline structure

Fig. 1 gives the XRD patterns of the hydrous zirconia supports and the catalysts. The crystalline structure of Zr-T samples varied distinctly with the hydrothermal temperature (Fig. 1a). No diffraction peak appeared in Zr-110, which was indicative of the amorphous state. As the hydrothermal temperature increased up to 150 °C, there appeared strong diffraction peaks of tetragonal phase and weak peaks of monoclinic phase. A further increase in the hydrothermal temperature to 200 °C led to increase in the diffraction peaks of monoclinic phase, but hydrous zirconia still mainly contained tetragonal phase. The phase compositions of the different samples were calculated according to the following

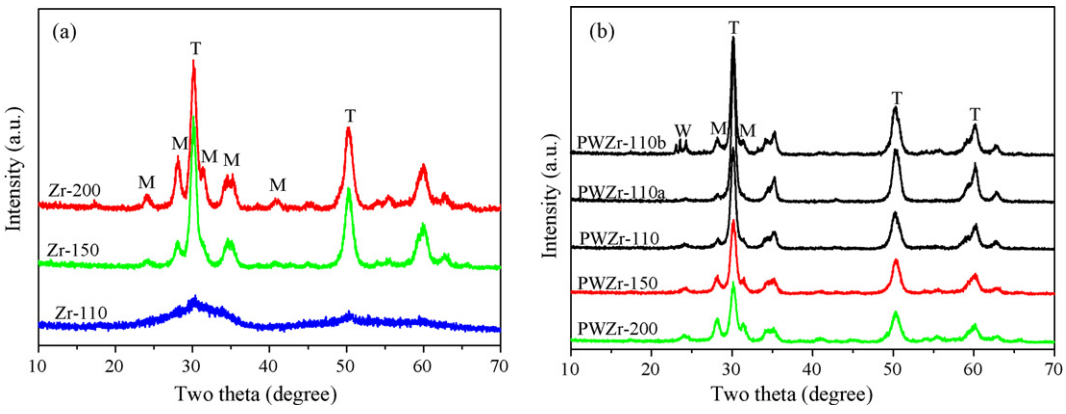

Fig. 1. XRD patterns of hydrous zirconia supports and PWZr-T catalysts (W-WO_3, M-monoclinic ZrO_2, and T-tetragonal ZrO_2).

Table 1
Fraction of tetragonal ZrO_2, pore structure and acidity of PWZr-T.

Sample	X_{TZ} (%)	X_{TWZ} (%)	S_{BET} (m^2/g)	Average pore diameter (nm)	Total volume (cm^3/g)
PWZr-110	–	87.0	69	14.1	0.29
PWZr-150	74.5	72.2	66	6.8	0.14
PWZr-200	62.8	58.7	71	7.3	0.16

X_{TZ} and X_{TZW} represent the tetragonal percentage of Zr-T and PWZr-T, respectively.

formula:

$$X_t = \frac{I_t}{I_{m1} + I_{m2} + I_t} \times 100$$

where I_t, I_{m1}, and I_{m2} represents the relative diffraction intensity of (1 0 1) plane of tetragonal zirconia, ($\bar{1}$ 1 1) plane and (1 1 1) plane of monoclinic zirconia, respectively. The calculated results are listed in Table 1. Apparently, the fraction of tetragonal phase in hydrous zirconia decreased from 74.5% for Zr-150 to 62.8% for Zr-200 as the hydrothermal temperature increased from 150 °C to 200 °C. The crystalline structure of the catalyst is shown in Table 1 and Fig. 1b. It could be seen that the fraction of tetragonal zirconia in the catalyst decreased from 87% for PWZr-110 to 58.7% for PWZr-200 as the hydrothermal temperature increased from 110 °C to 200 °C. As the calcination temperature after loading with W increased, the tetragonal zirconia slightly decreased. In addition, no diffraction peak of WO_3 was observed for the all the samples except that there appeared obvious WO_3 diffraction peak in PWZr-110b. It seemed that WO_3 crystallites existed only in PWZr-110b and tungsten oxide species in other samples were in the amorphous state of highly dispersion, regardless of amorphous or crystallized hydrous zirconia acting as support.

In fact, the X-ray diffraction lines would become too broad to be visible if the crystallite sizes are too small. The XRD result is inaccurate as the size of the crystallites was smaller than 5 nm, as proposed by Sahital et al. [17]. Therefore, XRD technology may be useless to determine the crystalline structure of too small crystallites, like WO_3 in our samples. Fortunately, Raman spectroscopy is sensitive to smaller WO_3 crystallites than XRD. In the present work, the catalysts were further characterized by Raman spectroscopy in order to clarify the state of tungsten oxide species on zirconia and the results are presented in Fig. 2. The Raman bands at 706–712 cm^{-1} and 810 cm^{-1} are generally assigned to the characteristic bands of WO_3 microcrystallites [3,4,18]. The band centering at 970–990 cm^{-1} is assigned to the stretching mode of W=O in highly distorted octahedral coordinated amorphous tungsten oxide species [4,19]. It could be clearly seen that there appeared Raman peaks at about 706–712 cm^{-1}, 810 cm^{-1} and 900–990 cm^{-1} for PWZr-200, PWZr-110b PWZr-110a and PWZr-110. The band at 810 cm^{-1} was stronger than that at 900–990 cm^{-1} for PWZr-200 and PWZr-110b, while the band at 900–990 cm^{-1} was stronger for the other samples. The intensity of Raman peak of WO_3 crystallites increased with the WO_3 loading [3]. Therefore, it could be inferred that PWZr-200 and PWZr-110b contained more WO_3 microcrystallites than other samples although both WO_3 microcrystallites and amorphous tungsten oxide species were present in all the catalysts.

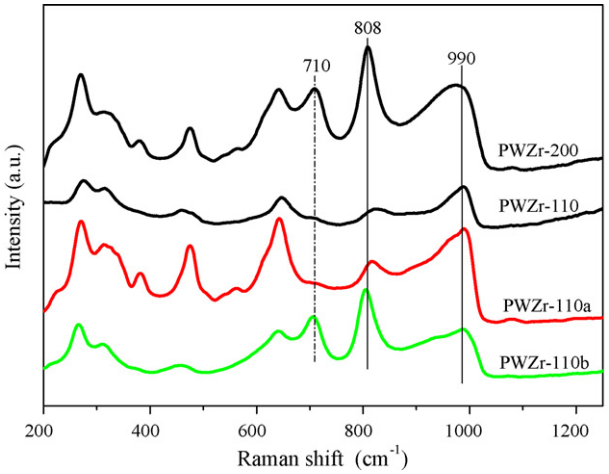

Fig. 2. Raman spectra of different catalysts.

3.2. Specific surface area and the pore structure

The specific surface area and the pore structure of PWZr-T catalysts were determined by the BET isothermal equation and BJH method, as shown in Table 1 and Fig. 3. All the PWZr-T samples possessed very similar surface areas, ca. 70 m^2/g. The pore volume of PWZr-110 was 0.29 cm^3/g, which was almost twice larger than that of both PWZr-150 (0.14 cm^3/g) or PWZr-200 (0.16 cm^3/g). The average pore diameter and pore size distribution of different samples also showed obvious difference. The average pore diameter of PWZr-110 was 14.1 nm, approximately twice as large as that of PWZr-150 (6.8 nm) or PWZr-200 (7.3 nm). Moreover, the pore size distribution of the former was wider than that of the latter. These findings suggested that the difference in the pore structure may be related to the crystallization of hydrous zirconia support. The crystallization of hydrous zirconia could generate the relatively stable pore structure. In fact, the pore size distribution of Zr-200 support was similar to that of PWZr-200 catalyst (not shown here). Therefore, it could be inferred that the pore structure of crystalline hydrous zirconia support played an important role in the determining the pore structure of the catalyst.

3.3. Reduction properties

The reduction properties of the catalysts were measured by H_2-TPR and the results are shown in Fig. 4. It could be seen from Fig. 4 that two very small reduction peaks appeared at low temperatures of 230 °C and 390 °C for all the samples. The first small peak may be associated with the reduction of Pt^{4+} and the second may be related to the partial reduction of WO_x. At a higher temperature of 720 °C, a not well resolved peak was observed at in the TPR profiles of PWZr-150 and PWZr-200 samples, while it was not visible for PWZr-110. A larger reduction peak at a higher temperature above 800 °C was observed for all the samples, which was attributed to the reduction of WO_x species strongly bond to the zirconia support [20]. The different reduction behaviors of the samples may be indicative of different states of tungsten oxide.

3.4. Surface acidity

The acidities of different catalysts were characterized by Py-IR method. The IR spectra are shown in Fig. 5 and the calculated data are listed in Table 2. Brønsted (B) acid sites appeared in the catalysts as indicated by the band at 1540–1547 cm^{-1}. Lewis (L) acid sites were also formed on the catalysts surface, characterized by the IR absorption bands at approximately 1445 cm^{-1} and 1610 cm^{-1}. The band corresponding to pyridine associated with both, Brønsted and

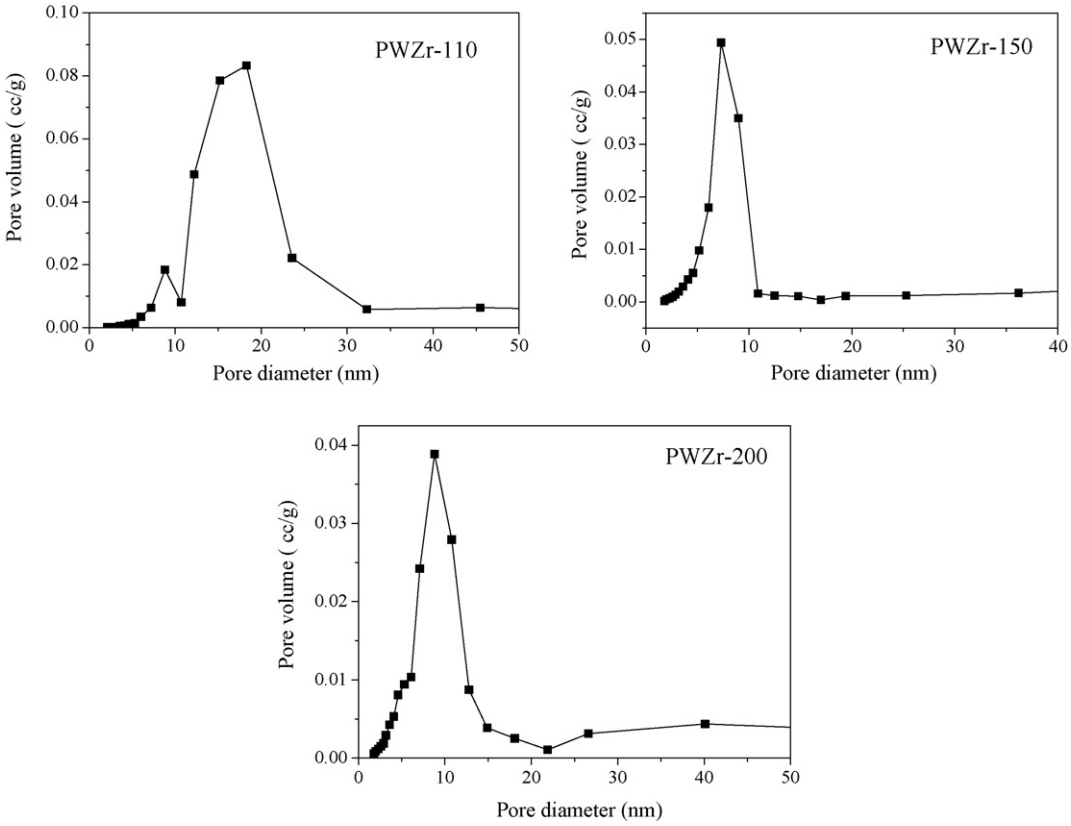

Fig. 3. Pore size distributions of Pt/WZr-T.

Lewis (B + L) acid sites, was also observed around 1490 cm^{-1}. The amount of weak B and L acid sites over PWZr-110 was 95.3 μmol/g and 52 μmol/g, respectively. The values were close to those over PWZr-200. PWZr-110b calcined at 800 °C possessed fewer weak B acid sites, while the amount of the weak L acid sites was similar to that over PWZr-110. As for the strong acid sites, it was obviously seen from Table 2 and Fig. 5 that strong B acid sites over all the samples could be almost negligible and the strong L acid over the samples were also relatively few, only 6.7 μmol/g for PWZr-110 and PWZr-200. The amount of strong L acid sites over PWZr-110b was fewer, only 3.7 μmol/g. As suggested by Boyse and Ko [18], a distinct decrease in the B and L acid sites over PWZr-110 may be related to the formation of considerable WO_3 microcrystallites.

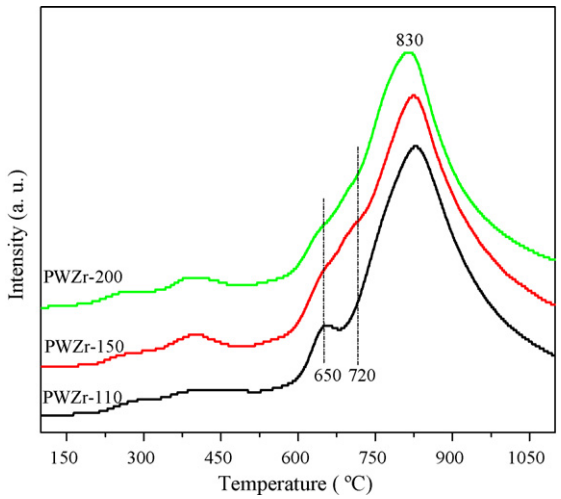

Fig. 4. H_2-TPR profiles of PWZr-T.

3.5. *n*-Hexane isomerization performance

The isomerization activity of the different catalysts was expressed as the yield of iso-hexanes, as shown in Fig. 6. The isomerization activity of different catalysts increased in such an order: PWZr-200 (PWZr-150) > PWZr-110b ≫ PWZr-110a ≥ PWZr-110. Obviously, the increase in the hydrothermal temperature led to a catalyst with high catalytic activity. In addition, at the low hydrothermal temperature, the enhancement of the calcination temperature of sample after loading W also resulted in the enhancement in the isomerization activity.

4. Discussion

Tungstated zirconia possessed super acidity and high catalytic activity only when amorphous hydrous zirconia was load with W [1]. From this point, Pt/WO_3–ZrO_2 should possess the lower catalytic activity when the crystalline hydrous zirconia was used as support. However, the present results showed that the catalyst PWZr-200 prepared by using crystallized Zr-200 as support existed much higher isomerization activity than PWZr-110 prepared by using amorphous Zr-110. It seemed that the crystalline

Table 2
Acidic properties of PWZr-T catalysts.

Sample	Weak acid site (μmol/g)^w		Strong acid site (μmol/g)^s	
	B	L	B	L
PWZr-110	95.3	52	0.2	6.8
PWZr-200	102.0	48.1	0.1	6.7
PWZr-110b	56.8	49.2	0.05	3.7

Weak acid site (μmol/g)^w: desorption at 150 °C; strong acid site (μmol/g)^s: desorption at 350 °C.
PWZr-110b: tungstated zirconia calcined at 800 °C.

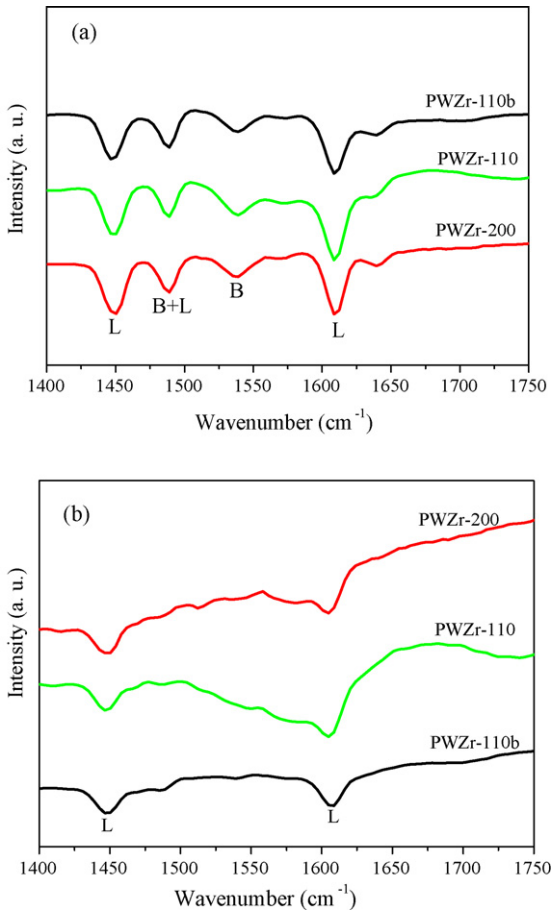

Fig. 5. Py-IR spectra of different catalysts. (a) Evacuation desorption at 150 °C and (b) evacuation desorption at 350 °C.

structure of hydrous zirconia support could not determine the catalytic activity. In addition, it could be seen from Table 1 and Fig. 1b that the fraction of tetragonal zirconia in PWZr-T decreased slightly with the increasing hydrothermal temperature, while the isomerization activity distinctly increased. It was generally thought that the tetragonal zirconia was active phase in tungstated zirconia for catalytic reaction. However, the present results showed that the presence of larger tetragonal zirconia in PWZr-T was not enough to obtain the high isomerization activity. The role of catalyst acidity in the isomerization reaction is also considered in the present work. The surface acidity of PWZr-110 and PWZr-200 is similar (Table 2 and Fig. 5), but the catalytic activity of PWZr-200 was much higher than that of PWZr-110. The sample PWZr-110b calcinated at 800 °C possessed fewer strong acid sites than that calcinated at 700 °C, while the former showed higher catalytic activity than the latter. The above results indicted that it was difficult to directly correlate the isomerization activity with the acidity of the catalyst, in agreement with the results from many researchers [3,12,21].

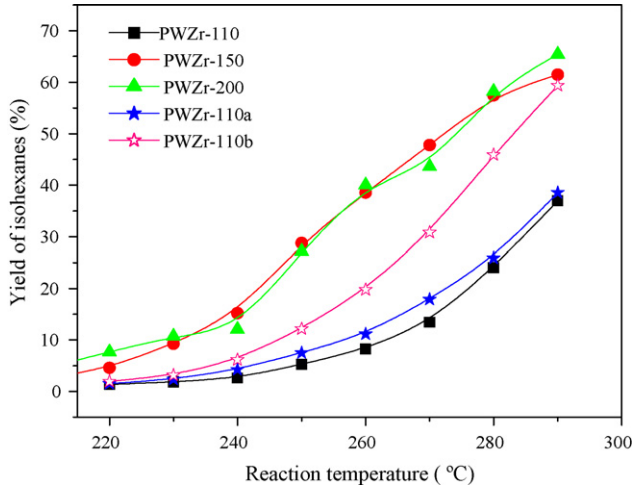

Fig. 6. Yields of iso-hexanes over PWZr-T.

In order to further elucidate the factor influencing the catalytic activity, the states of tungsten oxide species over different catalysts was considered. PWZr-200 contained more WO_3 microcrystallites and fewer amorphous tungsten oxide species than PWZr-110 and the former showed much higher catalytic activity than the latter. In addition, the enhancement in the calcination temperature of PWZr-110 from 700 °C to 800 °C led to the formation of considerable WO_3 microcrystallites. The catalytic activity also significantly increased with the calcination temperature. These findings allow us to believe that the presence of considerable WO_3 microcrystallites in catalyst was crucial to obtain the high isomerization activity. Moreover, Rossi et al. [15] also found that the removal of WO_3 crystallites from $Pd/WO_3–ZrO_2$ led to a substantial decrease of the isomerization activity. In addition, Vaudagna et al. [3,4] considered that the existence of WO_3 crystallites having optimum size and shape is necessary to partially reduce WO_x and stabilize the negative charge and high catalytic activity. These investigations strongly supported our proposal that the presence of considerable microcrystalline WO_3 in $Pt/WO_3–ZrO_2$ catalyst was essential for achieving high catalytic activity in the n-hexane isomerization reaction. Besides, WO_3 microcrystallites in the catalyst may participate in the building up strong acid sites by redox progress and stabilizing the intermediate oxidation states of tungsten [3]. Maybe, the strong acid sites generated under the reaction condition or in the ambience of H_2 would promote the isomerization reaction.

5. Conclusions

The hydrothermal temperature led to the change in the crystalline structure of hydrous zirconia support and the tungsten oxide species on the Pt-promoted tungstated zirconia catalyst, while no great change in the acidity of catalyst happened. The correlation between the isomerization activity, crystalline structure of hydrous zirconia support and the acidity of $Pt/WO_3–ZrO_2$ could not well be established. The state of tungsten oxide over the catalyst played a very important role in determining the isomerization activity of the catalyst. The existence of considerable WO_3 microcrystallites in $Pt/WO_3–ZrO_2$ was indispensable for achieving the high catalytic activity in n-hexane hydroisomerization.

Acknowledgements

We acknowledge the financial support of this work from the Ministry of Science and Technology of PR China (No. 2004CB720603) and Postdoctoral Science Foundation of PR China (200902221).

References

[1] K. Arata, M. Hino, J. Chem. Soc., Chem. Commun. (1988) 1259–1260.
[2] J.C. Yori, J.M. Parera, Catal. Lett. 65 (2000) 205–208.
[3] S.R. Vaudagna, S.A. Canavese, R.A. Comlli, N.S. Fígoli, Appl. Catal. A 168 (1998) 93–111.
[4] S.R. Vaudagna, R.A. Comelli, N.S. Fígoli, Appl. Catal. A 164 (1997) 265–280.
[5] J.C. Yori, C.R. Vera, J.M. Parera, Appl. Catal. A 163 (1997) 165–175.
[6] M. Hino, K. Arata, Appl. Catal. A 169 (1998) 151–155.
[7] M.A. Arribas, F. Márquez, A. Martínez, J. Catal. 190 (2000) 309–319.
[8] M.G. Falco, S.A. Canavese, N.S. Fígoli, Catal. Commun. 2 (2001) 207–211.

[9] C.C. Hwang, X.R. Chen, S.T. Wong, C.L. Chen, C.Y. Mou, Appl. Catal. A 323 (2007) 9–17.
[10] S.T. Wong, T. Li, S. Cheng, J.F. Lee, C.Y. Mou, J. Catal. 215 (2003) 45–56.
[11] Y.N. Huang, B.Y. Zhao, Y.C. Xie, Appl. Catal. A 172 (1998) 327–331.
[12] M.A. Cortés-Jácome, C. Angeles-Chavez, E. Lopez-Salinas, J. Navareete, P. Toribio, J.A. Toledo, Appl. Catal. A 318 (2007) 178–189.
[13] S. Kuba, P. Lukinskas, R.K. Grasselli, B.C. Gates, H. Knözinger, J. Catal. 216 (2003) 353–361.
[14] S. Kuba, P. Lukinskas, R. Ahmad, F.C. Jentoft, R.K. Grasselli, B.C. Gates, H. Knözinger, J. Catal. 219 (2003) 376–388.
[15] S.D. Rossi, G. Ferraris, M. Valigi, D. Gzaaoli, Appl. Catal. A 231 (2002) 173–184.
[16] Y.Q. Song, C.L. Kang, Y.L. Feng, F. Liu, X.L. Zhou, D.R. Yao, L.Y. Xu, Chin. J. Catal. 29 (2008) 1196–1198.
[17] S.R. Sashital, J.B. Cohen, R.L. Burwell, J.B. Butt, J. Catal. 50 (1977) 479–493.
[18] R.A. Boyse, E.I. Ko, J. Catal. 171 (1997) 191–207.
[19] J.A. Horsley, I.E. Wachs, J.M. Brown, G.H. Via, F.D. Hardcastle, J. Phys. Chem. 91 (1987) 4014–4020.
[20] V. Logie, P. Wehrer, A. Katrib, G. Maire, J. Catal. 189 (2000) 438–448.
[21] S. Kuba, P.C. Heydorn, R.K. Grasselli, B.C. Gates, M. Che, H. Knözinger, Phys. Chem. Chem. Phys. 3 (2001) 146–154.